

Review

Microorganism Assisted Synthesized Nanoparticles for Catalytic Applications

Xiaojiao Fang ^{1,2}, Yin Wang ², Zegao Wang ^{2,3}, Zaixing Jiang ^{1,*} and Mingdong Dong ^{2,*} 

¹ MIT Key Laboratory of Critical Materials Technology for New Energy Conversion and Storage, School of Chemistry and Chemical Engineering, State Key Laboratory of Urban Water Resource and Environment, Harbin Institute of Technology, Harbin 150001, China; fang@inano.au.dk

² Interdisciplinary Nanoscience Center (iNANO), Aarhus University, DK-8000 Aarhus C, Denmark; yin.wang@post.au.dk (Y.W.); wangzegao@gmail.com (Z.W.)

³ College of Materials Science and Engineering, Sichuan University, Chengdu 610065, China; wangzegao@gmail.com

* Correspondence: jzx1981@163.com (Z.J.); dong@inano.au.dk (M.D.); Tel.: +45-87156729 (M.D.)

Received: 28 November 2018; Accepted: 4 January 2019; Published: 8 January 2019



Abstract: Metal and metalloid nanoparticles (NPs) have attracted substantial attention from research communities over the past few decades. Traditional methodologies for NP fabrication have also been intensely explored. However, drawbacks such as the use of toxic agents and the high energy consumption involved in chemical and physical processes hinder their further application in various fields. It is well known that some bacteria are capable of binding and concentrating dissolved metal and metalloid ions, thereby detoxifying their environments. Bioinspired fabrication of NPs is environmentally friendly and inexpensive and requires only low energy consumption. Some biosynthesized NPs are usually used as heterogeneous catalysts in environmental remediation and show higher catalytic efficiency because of their enhanced biocompatibility, stability and large specific surface areas. Therefore, bacteria used as nanofactories can provide a novel approach for removing metal or metalloid ions and fabricating materials with unique properties. Even though a wide range of NPs have been biosynthesized, and their synthetic mechanisms have been proposed, some of these mechanisms are not known in detail. This review focuses on the synthesis and catalytic applications of NPs obtained using bacteria. The known mechanisms of bioreduction and prospects in the design of NPs for catalytic applications are also discussed.

Keywords: Nanoparticles; bacteria; synthetic mechanisms; catalytic applications

1. Introduction

Metal and metalloid NPs have shown some unique properties in many fields, such as catalysis, antimicrobial activity, drug delivery, cancer treatment, medical diagnostics, and nanosensors [1–6]. An increasing intense research effort has been devoted to metal and metalloid NPs in recent years. The conventional physical and chemical methods that are currently used to synthesize NPs have been developed over many years. However, the involvement of reductants and capping agents might result in the adsorption of toxic substances on the NPs [7–9].

Some microbes in nature are capable of fabricating NPs under ambient conditions without additional physical conditions or chemical agents [10]. As an alternative protocol, the biosynthesis of metal and metalloid NPs inspired by the biological paradigm has attracted substantial attention in the research community over the past few decades [11,12]. Among the biological methods, bacteria are a particularly important tool for fabricating NPs because of their variety and high adaptability to extreme conditions [13,14]. For example, toxic ions are usually harmful to the survival of microbes,

but some specific bacteria have evolved to be able to reduce or precipitate soluble toxic inorganic ions to insoluble and nontoxic metal NPs [15–17]. With regard to separating NPs from the remaining biomass of microorganisms, biphasic systems might be an efficient way. For example, Bi-NPs have been successfully separated with the use of an aqueous-organic partitioning system. The reductive ability of bacteria and the new technique in recovery of NPs provide an opportunity to fabricate NPs through a low-cost and easily manipulated process [18].

To date, many studies of the biosynthesis of NPs by bacteria, including elementary substances and compounds (as shown in Figure 1a), have been reported in the literature [19]. However, the exact reductive mechanisms are not yet fully understood. The mainstream view is that metal and metalloid NPs can be fabricated both intracellularly and extracellularly by bacteria. In an extracellular process, as shown in Figure 1b I and II, ions are reduced by proteins, enzymes and organic molecules in the medium or by cell wall components. Extracellular reduction appears to be more favorable than intracellular reduction, due to its lower cost, simpler extraction and higher efficiency. However, in the intracellular process, as shown in Figure 1b III, carboxyl groups located on the cell wall attract metal and metalloid ions by electrostatic interactions. Then, the ions enter the cells and interact with intracellular proteins and cofactors to produce NPs. In addition, many studies have shown that not only the living bacteria, but also the dead entities of some bacteria can also be used for biosynthesis of NPs. However, the mechanisms of these processes are different. Generally, the metabolic process may be responsible for the bioreduction of NPs in the living bacteria. However, for dead entities, metal and metalloid ions are bound to the bacteria cells that provide nucleation sites for NPs.

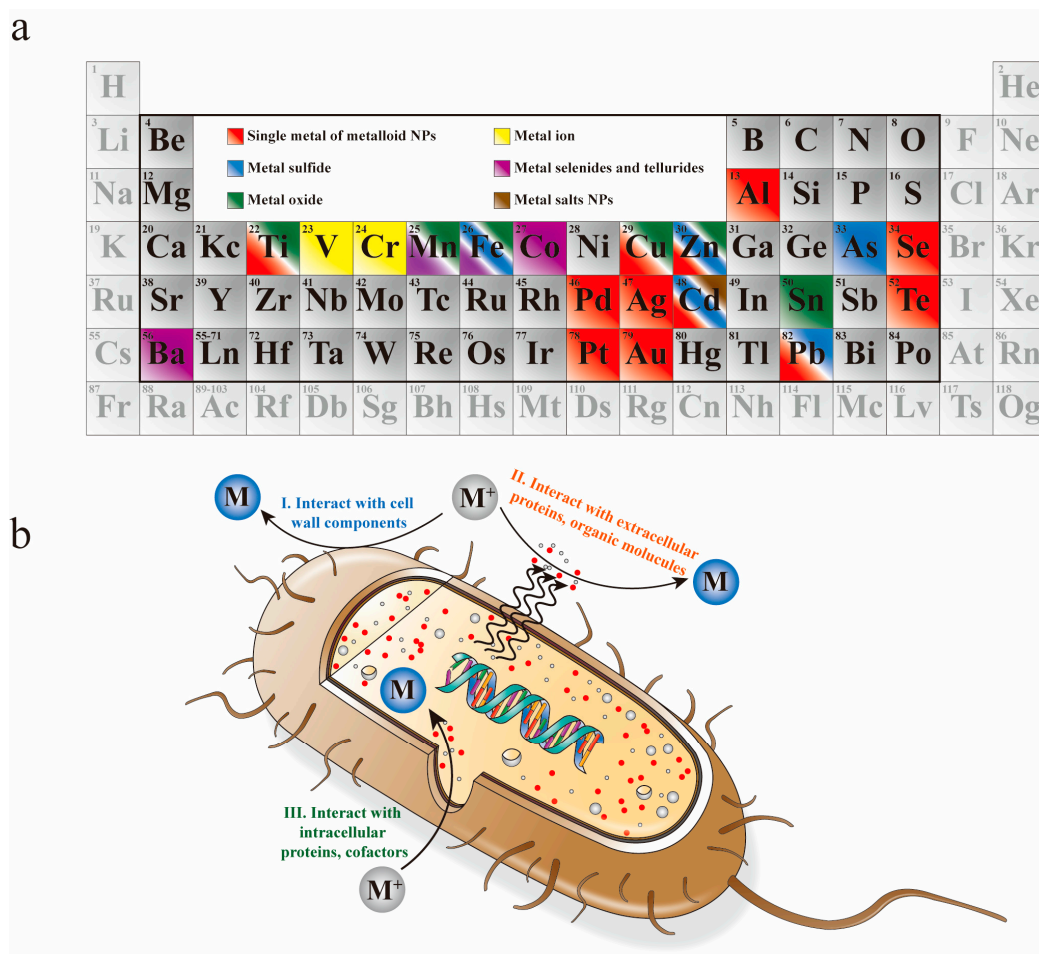


Figure 1. (a) Periodic table of elements that have been synthesized by bacteria. (b) Schematic representation of bacteria synthesis of NPs; both intracellular and extracellular process are included.

Regardless of the mechanism during the reduction of NPs, in most cases, the color of the culture changes because of localized surface plasmon resonance (LSPR). LSPR is a typical phenomenon that is considered the feedback of NP formation [20]. The coherent oscillation of electron gas at the surface of NPs is the origin of LSPR, leading to different colors. The intensity at a specific absorption wavelength in the UV-Vis spectrum is enhanced [21–23]. For characterization, multiple techniques can be applied to characterize the biosynthesized NPs. Scanning electron microscopy (SEM) and transmission electron microscopy (TEM) are robust approaches for elucidation of NPs morphology [24–27]. X-ray diffraction (XRD) is used to determine the crystal phase, and Fourier Transformed Infrared Spectroscopy (FT-IR) spectroscopy is carried out to identify the bio molecules that are responsible for the reduction and stabilization of the NPs.

Compared with NPs produced by conventional routes, biosynthesized NPs have some unique properties and can be employed with no side effect in fields such as the catalysis and degradation of organic pollutants [28,29]. In actual practice, the high efficiency of these NPs can usually be attributed to the high specific surface area when the particle size is reduced to the nanoscale [30]. Moreover, due to heterogeneity, the NPs can be separated from the substrate to enable their reuse, achieving the desired low cost and sustainability [31].

In this review, we survey the biosynthesized NPs obtained through different mechanisms for different bacteria. Additionally, the catalytic applications of some NPs obtained by different biological synthesis are discussed.

2. Biosynthesis of NPs

While it is well known that metal ions in a liquid solution are usually harmful to biological organisms, including microbes, some special bacteria have evolved the ability to inhibit diffusion of metal ions by reducing metal ions to NPs. From the perspective of synthesis, this provides a good opportunity to employ bacteria to fabricate particles at the nanoscale. NPs, including single metal, metalloid and related compounds, can be formed and harvested by biosynthesis due to bacterial resistance [32,33]. Regarding the details of the bioreduction mechanisms, some hypotheses have been proposed and proved based on various experimental results. This section will focus on the biosynthesis of NPs and the intrinsic mechanism by investigating living bacteria and cell-free extracts.

2.1. Elementary Substances

2.1.1. Single Metal

Compared with NPs fabricated by conventional approaches, biosynthesized metal NPs have better stability and oxidation resistance and have been applied in various fields [34].

In the bioreduction process, some enzymes play an important role in transporting electrons from certain donors to positive metal ion [35,36]. These enzymes are also considered to be responsible for the stabilization of the resultant NPs [37]. Ghiuta et al. employed two *Bacillus* species, namely, *Bacillus amyloliquefaciens* and *Bacillus subtilis*, to synthesize Ag-NPs. The well-defined Ag-NPs were distributed within quite a narrow size range in both cases. The authors believed that the alpha-amylase enzyme could control the size of Ag-NPs in a narrow range, and it is well known that both of these bacteria can generate the alpha-amylase enzyme [38,39]. Mishra et al. found that the *Stenotrophomonas* sp. BHU-S7, which was previously known as *Pseudomonas maltophilia*, could biosynthesize spherical Ag-NPs extracellularly. As shown in Figure 2a, the average size of these NPs is approximately 12 nm. The most widely accepted mechanism is that the extracellular enzymes, such as nitrate reductase enzyme, that appear in the supernatant facilitate electron transfer to Ag⁺ ions, resulting in the formation of Ag-NPs. They also proposed that the carbonyl groups of some proteins and enzymes could stabilize the Ag-NPs by binding to the NP surfaces [40].

Many researchers have reported that some functional groups, such as –NH₂, –OH, –SH and –COOH, of the proteins secreted by bacteria, play important roles in the reduction and stabilization of

NPs. These functional groups provide binding sites for fixing of metal ions, followed by the reduction of the metal ions outside the cells on the cell wall or in the periplasmic space. Li et al. reported the preparation of gold nanoparticles (Au-NPs) via protein extracts of *Deinococcus radiodurans*. In this study, protein functional groups such as $-\text{NH}_2$, $-\text{OH}$, $-\text{SH}$ and $-\text{COOH}$ act as binding sites to facilitate the reduction of Au^{3+} to Au-NPs [41,42]. Furthermore, it was found that in the subsequent stabilization process, these proteins encapsulated the Au-NPs as capping agents to prevent NPs from aggregating (as shown in Figure 2b). Two years later, the same group prepared Ag-NPs and Au-Ag bimetallic NPs by using the same bacteria. The authors attributed the reduction of the metal ions to the same mechanism as that described in their previous work. However, unlike the two-step reduction of gold ions (I. $\text{Au}^{3+} \rightarrow \text{Au}^+$, II. $\text{Au}^+ \rightarrow \text{Au-NPs}$), Ag^{1+} was reduced to Ag-NPs in a single step. Zeta potential value measurements confirmed that the Ag-NPs were more stable than Au-NPs [43–45].

The cytochrome protein is the basis for another important approach for reducing metal ions to NPs. The pigment produced by *Chryseobacterium artocarpi* CECT 8497 has been successfully used to generate coexisting spherical and irregular Ag-NPs. While the mechanism has not been elucidated, the FTIR spectroscopy showed the existence of strong chelation between the ester carbonyl group of flexirubin and Ag-NPs [46]. Lv et al. biosynthesized Cu-NPs extracellularly with *Shewanella loihica* PV-4. They showed that cytoplasm components, such as NADH/NADPH, vitamins and organic acids, acted as electron donors to reduce Cu^{2+} . Cytochrome c for electron transfer was the primary reductive factor [47].

In addition to using the bacteria themselves, biosynthesis of NPs can also be achieved by metabolites of bacteria with ongoing investigations of the mechanism of this process. Abirami et al. described the biosynthesis of Ag-NPs using *Streptomyces ghanaensis* VITHM1, and the major secondary metabolites were confirmed by gas chromatography-mass spectrography analysis. All the compounds might be involved in the reduction of Ag^+ to Ag^0 and stabilization of the NPs. The authors proposed that the reduction of the Ag^+ could be attributed to the hydroxyl group, while the carbonyl group was responsible for the stabilization of Ag-NPs. No precipitation occurred after the formation of Ag-NPs in solution for six months at room temperature [48].

Furthermore, based on the detected products, a novel mechanism that was different from the mechanism described above was also proposed. *Shewanella oneidensis* MR1 from anaerobic metal-reducing bacteria was used for the bioreduction of Cu^{2+} (as shown in Figure 2c), and the process was conducted with lactate as an electron donor. The authors proposed three possible mechanisms: an unidentified reductase in periplasm and cytoplasm can reduce Cu^{2+} to Cu^0 ; bioreduction can occur in the periplasm or cytoplasm, and membrane damage due to the toxicity of Cu may promote the transport of NPs across the cytoplasmic membrane; Cu^{2+} can be reduced to Cu^+ in the cytoplasm, and then Cu^+ can be disproportionated to form Cu^{2+} and Cu [49]. Pd-NPs can be prepared both intracellularly and extracellularly from Na_2PdCl_4 by *Enterococcus faecalis* with sodium formate as the electron donor (the NPs are shown in Figure 2d). The mechanisms of the Pd^{2+} diffusion into cells are still unknown, but the reduction mechanism, which was previously poorly understood, was partially identified by changing the pH during the reduction process [50]. The results showed that the reduction of Pd^{2+} mainly occurred in the chemical reaction of the ion-exchange process. A recent study proved that sunlight can also be used for catalytic biosynthesis of Ag-NPs with endophytic strain SYSU 333150. In the presence of sunlight, the reduction time decreased from 3 h to 4 min. Electron-hole pairs produced by excited molecules were transferred to free radicals and the excess electrons of surface-adsorbed reducing agent, resulting in neutralized Ag-NPs [51].

2.1.2. Metalloid Elements

Se^{2+} and Te^{2+} are toxic species that pose health and environmental risks [52,53]. While chemical removal of Se^{2+} and Te^{2+} often involves the use of dangerous reductants, bioinspired methods offer good opportunities for simultaneous decontamination and nanomaterials production [54–56]. Presentato et al. aerobically produced Se-NPs and Se nanorods (NRs) with *Actinomyces Rhodococcus*

aetherivorans BCP1. They proved that these bacteria have a high tolerance towards SeO_3^{2-} (500 mM), with the morphology of the final product being determined by the initial concentration of the precursor. The authors ascribed this reduction to the LaMer mechanism, where neutral Se atoms assembled into Se-nucleation seeds after they were reduced from SeO_3^{2-} , and Se-NPs formed via a ripening process. Se atoms were dissolved and released spontaneously because of the high free energy and low stability of Se-NPs in suspension. Subsequently, Se atoms might be precipitated as nanocrystals in one direction to form Se-NRs [57]. Aerobic biosynthesis of monodispersed nanosized Se-NPs was completed both intracellularly and extracellularly with *Enterobacter cloacae* Z0206. Large-scale proteomic analysis (iTRAQ) showed that the function of fumarate reductase was promoted by adding selenite. The probable mechanism was that *E. cloacae* Z0206 contains selenite-reducing factor, which is a special fumarate reductase [58]. Theoretically, selenite reduction anaerobically should be faster and more prominent than that under aerobic conditions. As an increasing number of bacteria species have been examined in NPs biosynthesis, some bacteria have been proved to be capable of reducing Se-NPs under aerobic and anaerobic conditions [59]. *Citrobacter freundii* Y9 has been used to produce Se-NPs (shown in Figure 2e). The anaerobic mechanism involved the reduction of selenite and its incorporation into organic products in an assimilatory process, or acting as electron acceptors in a dissimilatory process. The mechanisms under aerobic conditions are not well understood [60]. Avendaño et al. obtained Se-NPs by using *Pseudomonas putida*. The proposed mechanism was a two-step process involving the chelation of SeO_3^{2-} by thiol-containing molecules followed by the formation of selenodiglutathione. It is known that selenodiglutathione is the substrate of glutathione reductase, which produces unstable intermediates. As a result, the compound was converted to Se^0 . *Pseudomonasputida* is a strictly aerobic species, and no substrate other than oxygen serves as the final electron acceptor. Both selenite and selenate were added to the medium, and it was found that *P. putida* has no effect on the selenate at all [61].

In a recent study, Zonaro et al. biosynthesized Se-NPs and Te-NPs with reducing bacterial strains isolated from polluted sites, namely, *Stenotrophomonas maltophilia* SeITE02 and *Ochrobactrum* sp. MPV1. Both Se-NPs and Te-NPs were well dispersed and had spherical shapes. It is interesting that, unlike other biosynthesized metal NPs, Se-NPs increase in diameter with increasing incubation time, but the size of Te-NPs was quite stable [62]. Srivastava et al. biosynthesized hexagonal needle-shaped Te-NPs intracellularly with an aspect ratio of 1:4.4 (the Te morphology is shown in Figure 2f). Generally, the primary defense against metal and metalloid toxicity is an increased efflux or a decreased influx of the ions; however, tellurium resistance requires either volatilization or reductive precipitation of tellurite [63]. The NADH-dependent tellurite reductase may be responsible for the detoxification of tellurite to black Te-NPs [64].

Some of the elementary substances that have been synthesized by bacteria are listed in Table 1.

Table 1. Elementary substances synthesized by bacteria.

NPs	Cellular	Shape	Size	Type of bacteria	Ref.
Ag	Extra-	Spherical NPs	6~16 nm	<i>Pseudomonas putida</i> MVP2	[12]
	Extra-	Spherical NPs	198~595 nm	<i>Streptomyces</i> sp. 09 PBT 005	[24]
	Extra-	Spherical NPs	4.4 nm	<i>Exiguobacterium</i> sp. KNU1	[26]
	Extra-	Spherical NPs	140 nm	<i>Bacillus</i> species	[38]
	Extra-	Spherical NPs	12 nm	<i>Stenotrophomonas</i> sp. BHU-S7	[40]
	Extra-	Spherical NPs	30~50 nm	<i>Streptomyces ghanaensis</i> VITHM1	[48]
	Intra-	Equilateral triangles, hexagons NPs	200 nm	<i>Pseudomonas stutzeri</i> AG259	[36]
	Intra-	NA	15~500 nm	<i>Lactobacillus</i>	[44]
	NA	NA	37.13 ± 5.97 nm	<i>Deinococcusradiodurans</i>	[41]
	NA	Spherical NPs	2~11 nm	<i>Shewanellaoneidensis</i> MR-1	[45]
	NA	Spherical and irregular NPs	49 nm	<i>Chryseobacteriummartocarpi</i> CECT 8497	[46]
	NA	Spherical NPs	11~40 nm	<i>Endophytic Bacteria</i>	[51]

Table 1. Cont.

NPs	Cellular	Shape	Size	Type of bacteria	Ref.
Au	Intra-	NA	20~50 nm	<i>Lactobacillus</i>	[44]
	NA	Spherical NPs	10 ± 2 nm	<i>cinetobacter</i> sp. SW 30	[42]
	NA	NA	51.72 ± 7.38 nm	<i>Deinococcusradiodurans</i>	[41]
Au-Ag	Intra-	NA	100~300 nm	<i>Lactobacillus</i>	[44]
Cu	Intra-	Spherical NPs	20~40 nm	<i>Shewanellaoneidensis</i> MR1	[49]
	Extra-	Spherical NPs	10~16 nm	<i>Shewanellaloihica</i> PV-4	[47]
Pd	Intra- & Extra-	NA	< 10 nm	<i>Enterococcus faecalis</i>	[50]
Pb	Intra-	Spherical NPs	3~8 nm	<i>Shewanella</i> sp. KR-12	[19]
Bi	Intra-	Irregular NPs	< 150 nm	<i>Serratia marcescens</i>	[18]
Se	Extra-	Spherical NPs	50~500 nm	<i>Actinomycete Rhodococcus aetherivorans</i>	[57]
	Extra-	Spherical NPs	100~500 nm	<i>Pseudomonas putida</i>	[61]
	Intra-	Spherical NPs	104.6 ± 8.4 nm	<i>Shewanellaoneidensis</i> MR-1	[52]
	Intra- & Extra-	Rods	100~300 nm	<i>Enterobacter cloacae</i> Z0206	[58]
	Intra- & Extra-	Amorphous NPs	580 ± 109 nm	<i>Citrobacter freundii</i> Y9	[60]
	NA	Amorphous	100 ± 10 nm 6 h: 221.1 nm, 24 h: 345.2 nm, 48 h: 357.1 nm	<i>cinetobacter</i> sp. SW 30	[42]
Te	NA	NA	100~300 nm	<i>Stenotrophomona smaltophilia</i> SeITE02	[62]
	Intra-	Hexagonal needle-shaped NPs	diameter: 10 nm, length: 44 nm 6 h: 78.5 nm, 24 h: 76.2 nm, 48 h: 76.1 nm	<i>Halococcus salifodinae</i> BK3	[64]
	NA	Rods	diameter: 22 nm, length: 185 nm	<i>Pseudomonas</i> sp	[53]

NA: Not Available.

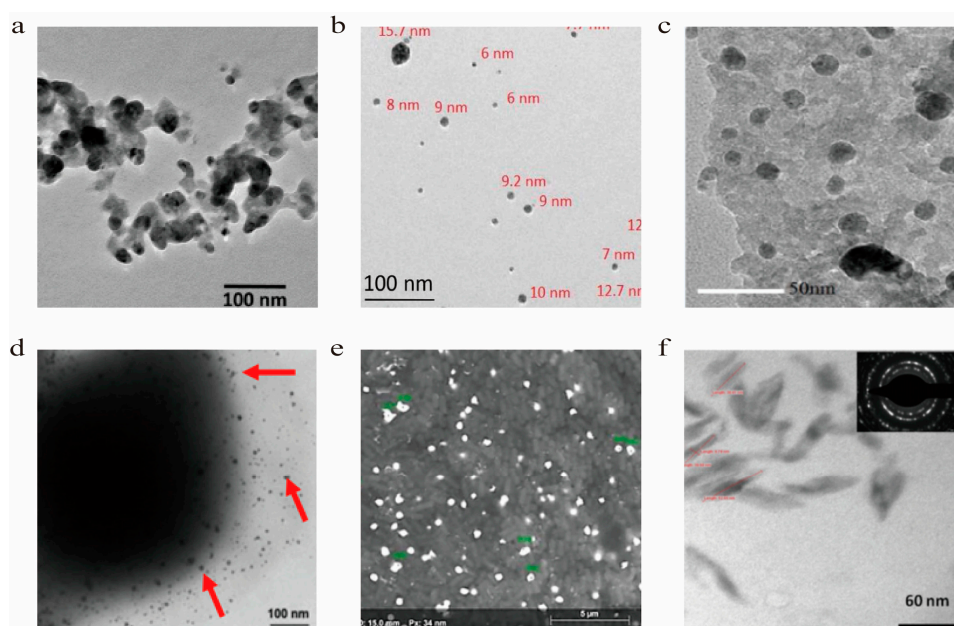


Figure 2. SEM and TEM images of biosynthesized elementary substance. (a) Ag-NPs by *Bacillus* sp. SBT8, scale bar: 100 nm (reprint from [39] with permission from Taylor & Francis. Copyright 2018); (b) Au-NPs by *Acinetobacter* sp. SW 30, scale bar: 100 nm (reprint from [42] with permission from Elsevier. Copyright 2018); (c) Cu-NPs by *Shewanella loihica* PV-4, scale bar: 50 nm (reprint from [47] with permission from Elsevier. Copyright 2018); (d) Pd-NPs by *Enterococcus Faecalis*, scale bar: 100 nm (reprint from [50] with permission from Elsevier. Copyright 2016); (e) Se-NPs by *Lactobacillus casei* 393, scale bar: 5 μm (reprint from [59] with permission from Elsevier. Copyright 2018); (f) Te-NPs by *Haloarchaeon Halococcus Salifodinae* BK3, scale bar: 60 nm (reprint from [63] with permission from Springer Nature. Copyright 2015).

2.2. Compounds

Wastewater discharge, including metal ions from industrial and commercial sources, has adverse effects on the environment and humans [65]. These metal pollutants can also be considered a resource for recycling and production of valuable materials such as metal oxides, metal sulfides or other materials, through a biological enrichment procedure [66].

2.2.1. Metal Oxide

The mechanisms involved in the bioreduction of metal oxides are similar to those of single metals, and proteins secreted by bacteria are the most common reductants. For example, magnetic Fe₃O₄-NPs can be produced intracellularly by *Magnetospirillum magneticum* with FeCl₃ as precursor. It was shown that the intracellular magnetosomes organelles of *Magnetospirillum magneticum* play a vital role in the formation of Fe₃O₄-NPs. The magnetosomes are encapsulated by the globular protein complex named ferritin that contains 24 subunits. Because of this (as shown in Figure 3a), Fe can be stored in a nontoxic and soluble form. The formation of Fe₃O₄-NPs and nucleation of the minerals may be attributed to these proteins [67].

Metabolites can also act as reductants. Crystalline hexagonal α -Fe₂O₃-NPs capped with protein were biosynthesized with *Bacillus cereus* SVK1 under ambient conditions. In this case, FeCl₃ was also used as the precursor. The metabolites secreted by the bacteria in the culture broth induced the reduction and stabilization process of metal NPs (as shown in Figure 3b) [68,69].

Some special enzymes have been confirmed to have the ability of biosynthesizing NPs. Srivastava et al. produced SnO₂-NPs using *Erwinia herbicola*. The biosynthesized SnO₂-NPs were either crystalline or amorphous (as shown in Figure 3c), depending on whether a heating process was used after biosynthesis. The general process for the formation of SnO₂ is that the enzymes secreted by bacterial cells trapped the Sn²⁺, and then the reduction process was initiated by transferring electrons to Sn²⁺. To generate Sn-NPs, Sn²⁺ gained two electrons from certain enzymes such as NADH that were oxidized at the same time. Subsequently, the Sn-NPs were oxidized to SnO₂-NPs because of the oxygen in solution [70].

In addition, CuO-NPs were reported to be produced by *Morganella morganii* bacteria for the first time, as shown in Figure 3d the size of the obtained particles was less than 10 nm, but the exact mechanisms are unknown [71].

2.2.2. Metal Chalcogenides

Metal chalcogenides have attracted increasing interest as new semiconductor materials because of their favorable band structure [72,73]. In the regard of their bioreduction, proteins play important roles. Sakimoto et al. used a nonphoto-synthetic CO₂-reducing bacterium *Moorella thermoacetica* to extracellularly precipitate CdS-NPs (as shown in Figure 3e). The CdS-NPs were formed after adding Cd(NO₃)₂ solution into a specific growth culture, which contains glucose-grown cells and Cys. Furthermore, the authors found that *Moorella thermoacetica* could subsequently carry out photosynthesis to reduce CO₂ in the presence of CdS-NPs that donate photogenerated electrons. The photosynthesis process converted CO₂ to acetic acid. This study paved the way for a new approach to solar-to-chemical synthesis [74]. In another example, the anaerobic sulfate-reducing bacteria *Desulfovibrio caledoniensis* was used both intracellularly and extracellularly for biosynthesis of CdS-NPs without any other sulfide source agents (as shown in Figure 3f). The process was as follows: I. ATP sulfurylase activated anaerobic reduction of sulfate in bacteria; II. ferredoxin or NADH reduced the resultant adenosine-phosphosulfate (APS) complex to sulfite; III. assimilatory or dissimilatory sulfite reductase reduced sulfite to sulfide [75]. Kominkova et al. biosynthesized CdTe-QDs by *Escherichia coli* using CdCl₂ and Na₂TeO₃ as the precursors. The bacteria secreted extracellular proteins to bind the metals. As a result, the nucleated nanocrystals formed extracellularly after the incubation of the bacteria and precursors. Then, nanocrystals were enlarged and interconnected, leading to the formation of QDs. It is

possible that the proteins or peptides involved in this process were thiols, such as glutathione [76]. Pb is an environmental toxin due to its strong accumulative ability. Yue et al. biosynthesized highly pure PbS nanocrystals extracellularly by regulating the concentration of polyethylene glycol in the *Clostridiaceae* sp. system (as shown in Figure 3g). The probable mechanism was that SO_4^{2-} was first reduced to S^{2-} by the sulfate-reducing bacteria, and then S^{2-} gradually combined with Pb^{2+} to precipitate as PbS-NPs [77].

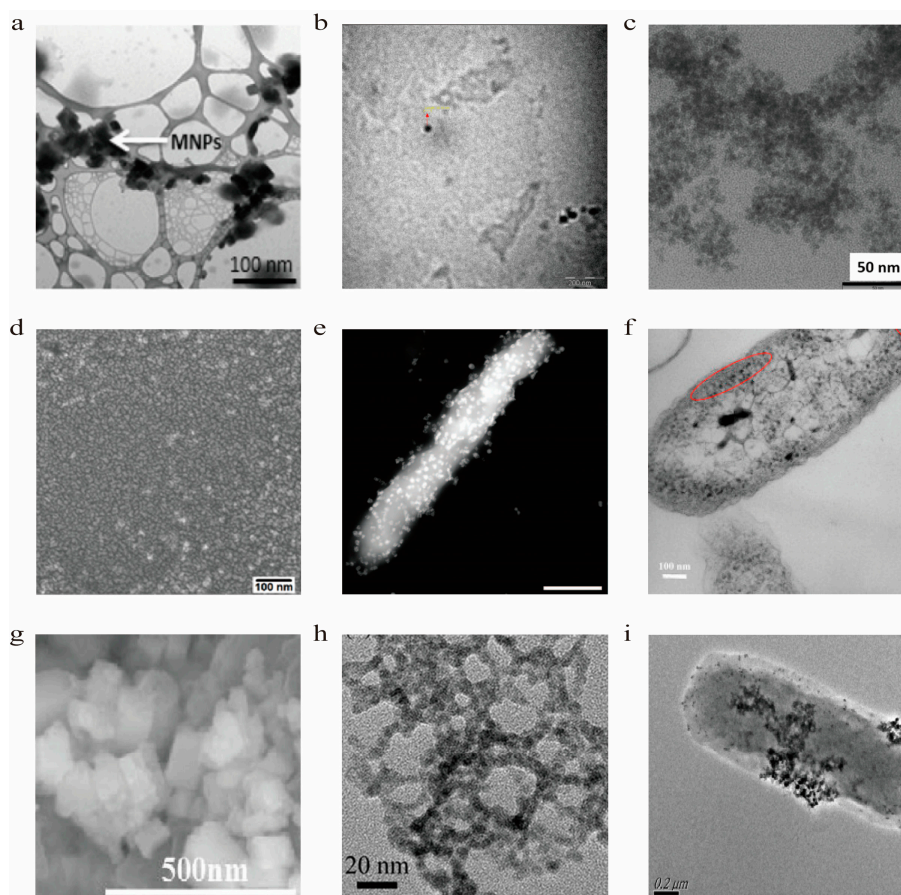


Figure 3. SEM and TEM images of biosynthesized compounds. (a) Fe_3O_4 by *Luteinizing Hormone Releasing Hormone*, scale bar: 100 nm (reprint from [67] with permission from Elsevier. Copyright 2015); (b) Fe_2O_3 by *Bacillus cereus* SVK1, scale bar: 50 nm (reprint from [68] with permission from Elsevier. Copyright 2015); (c) SnO_2 by *Erwinia Herbicola*, scale bar: 50 nm (reprint from [70] with permission from the American Chemical Society. Copyright 2014); (d) CuO by *Morganela morganii*, scale bar: 100 nm (reprint from [71] with permission from Elsevier. Copyright 2017); (e) CdS by *Moorella thermoacetica*, scale bar: 500 nm (reprint from [74] with permission from American Association for the Advancement of Science. Copyright 2016); (f) CdS by *Desulforibrio caledoiensis*, scale bar: 100 nm (reprint from [75] with permission from Elsevier. Copyright 2016); (g) PbS by *sulfate-reducing bacteria*, scale bar: 500 nm (reprint from [77] with permission from Springer Nature. Copyright 2016); (h) CuS by *Shewanella Oneidensis* MR-1, scale bar: 20 nm (reprint from [80] with permission from Elsevier. Copyright 2016); and (i) ZnS by *Shewanella Oneidensis* MR-1, scale bar: 0.2 μm (reprint from [81] with permission from Elsevier. Copyright 2015).

Studies have also confirmed the reductive ability of some substances secreted by bacteria. Biosynthesis of PbS_2 -NPs was first reported by Srivastava et al., who synthesized spherical β - PbS_2 -NPs intracellularly with *Idiomarina* sp. strain PR58-8). When toxic Pb^{2+} was taken up by the bacteria, the amount of nonprotein thiols increased in a dose dependent manner. It is possible that the thiols were responsible for the Pb^{2+} detoxification and growth of the PbS_2 crystals [78]. *Shewanella oneidensis*

MR-1 can be used for the biosynthesis of many different types of NPs [79]. Zhou et al. used it to synthesize hydrophilic CuS-NPs extracellularly (as shown in Figure 3h). $\text{Na}_2\text{S}_2\text{O}_3$ and CuCl_2 were used as precursors. *S. oneidensis* is well known for accumulating S^{2-} in a reducing medium, and making $\text{S}_2\text{O}_3^{2-}$ an electron acceptor in this case. Therefore, it was understandable that CuS-NPs formed after the addition of Cu^{2+} [80]. ZnS-NPs were synthesized with the same bacteria under anaerobic conditions. It can be observed from Figure 3i that NPs mainly aggregated on the cell surface and in the medium. The probable mechanism was that the thiosulfate was reduced to S^{2-} in the periplasm of the bacteria, and then Zn^{2+} was precipitated in the presence of S^{2-} to form ZnS-NPs [81,82].

Some of the compounds that have been synthesized by bacteria are listed in Table 2.

Table 2. Compounds synthesized by bacteria.

NPs	Cellular	Shape	Size	Type of Bacteria	Ref.
Fe_3O_4	Intra-	Cuboidal, rectangular and spherical NPs	10~60 nm	<i>Magnetospirillum magneticum</i>	[67]
SnO_2	Extra-	Spherical and tetragonal NPs	15~40 nm	<i>Erwinia herbicola</i>	[70]
Fe_2O_3	NA	Spherical NPs	30.2 nm	<i>Bacillus cereus</i> SVK1	[68]
CuO	NA	Orthorhombic NPs	<10 nm	<i>Morganelamorganii</i> bacteria	[71]
	Extra-	Cubic NPs	2~10 nm	<i>Bacillus licheniformis</i>	[72]
CdS	Intra- & Extra-	Spherical NPs	40~50 nm	<i>Desulforibrio caledoiensis</i>	[75]
	NA	Spherical NPs	10 nm	<i>Escherichia coli</i>	[73]
PbS	Extra-	Cubic NPs	$50 \times 50 \times 100$ nm	<i>Clostridiaceae</i> sp	[77]
PbS_2	Intra-	Spherical NPs	6 nm	<i>Idiomarina</i> sp. Strain PR58-8	[78]
CuS	Extra-	Spherical NPs	5 nm	<i>Shewanella oneidensis</i> MR-1	[80]
ZnS	Extra-	Spherical NPs	5 nm	<i>Shewanella oneidensis</i> MR-1	[81]
CdSe	Intra-	NA	3.3 ± 0.6 nm	<i>Shewanella oneidensis</i> MR-1	[52]
CdTe	Extra-	NA	62 nm	<i>Escherichia coli</i>	[76]

NA: Not Available.

3. Catalytic Applications

Some biosynthesized NPs play the role of catalysts to remove specific pollutants, drawing the interest of the research community in recent years. Production and overuse of synthetic dyes, pesticides and pharmaceuticals have resulted in the pollution of water and soil [83,84]. Polluted wastewater and soil usually contain a large quantity of heavy metals and metalloids generated during industrial processes that pose a threat to the environment [85,86]. However, alternatively, the waste can also be utilized as a resource to fabricate NPs through the biological pathway for the degradation of specific pollutants [87–89]. In this section, we will review the catalytic applications of biosynthesized NPs (as shown in Figure 4).

3.1. Degradation of Dyes

Dyes are hazardous to almost all living organisms because of their tendency to eutrophication or due to their toxicity. Many industries, such as the food-processing, drug and textile industries, extensively use dyes that have given rise to severe pollution in water and soil. Some methods have been used to remove the residual dye in the industrial process, but the results have not been satisfactory. The low efficiency of the removal remains the main problem for this approach. By contrast, biosynthesized NPs exhibit an excellent catalytic performance because of their higher specific surface area and the greater number of active sites compared with polycrystalline materials. Yue et al. investigated the photocatalytic performance of biosynthesized PbS nanocrystals with different morphologies, such as nanocuboids, nanosheets and NPs. They confirmed that PbS acted as the oxidizer and electron capture agent in the degradation of methylene blue in the presence of H_2O_2 . PbS nanocuboids have the smallest specific surface area and show the best dye-removal performance. It has been speculated that (200) crystal plane was the main factor that influenced the

catalytic activities of PbS nanocuboids. Srivastava et al. evaluated the photocatalytic efficiency of biosynthesized SnO_2 -NPs in the degradation of dyes (shown in Figure 5). The three plots are the absorption spectra for photocatalytic degradation of three dyes (methylene blue, methyl orange, and Erichrome black T) at different time intervals. The SnO_2 -NPs showed excellent catalytic performance, with approximately 93.3%, 94.0% and 97.8% of methylene blue, methyl orange, and Erichrome black T degraded, respectively. Moreover, the SnO_2 -NPs can be easily separated from the reaction mixture by a simple centrifugation after the photocatalytic degradation reaction.

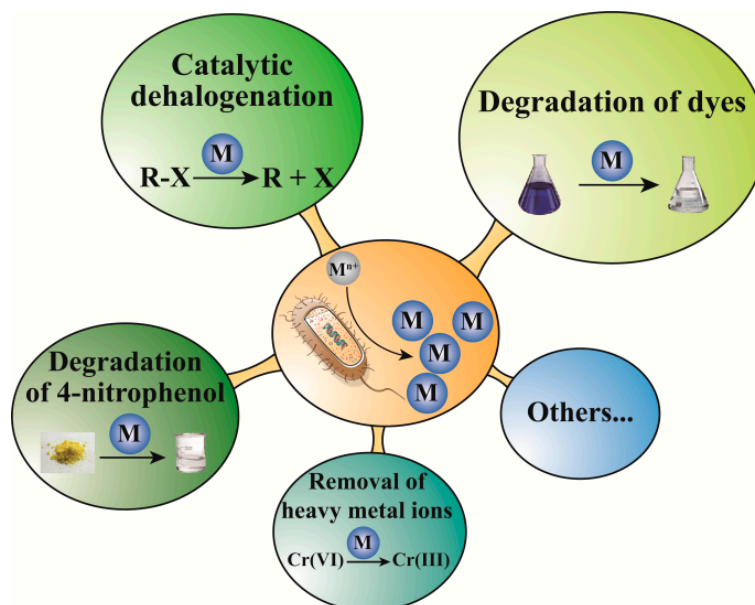


Figure 4. Catalytic applications of biosynthesized NPs, both elementary substances and compounds are included.

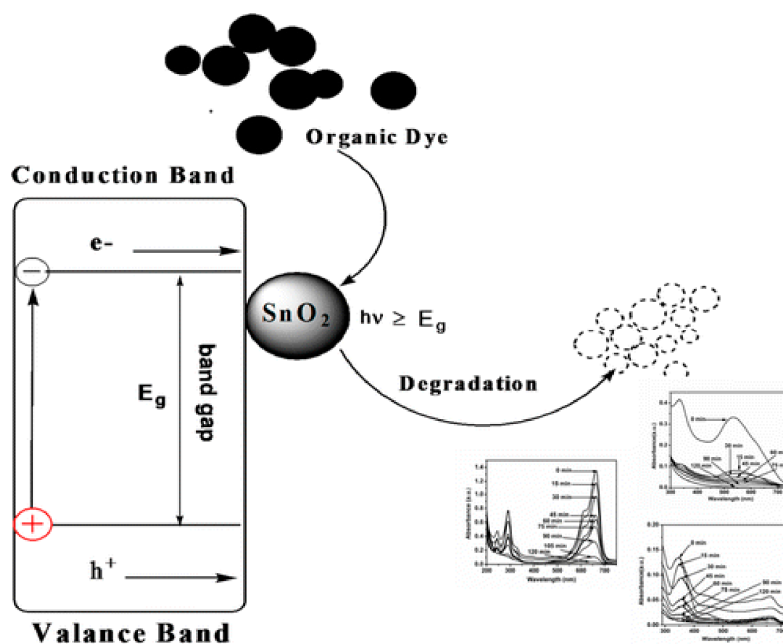


Figure 5. Schematic representation of the photocatalytic degradation process of dyes using SnO_2 nanoparticles (reprint from [70] with permission from the American Chemical Society. Copyright 2014).

Rhb is a special dye that is resistant to biodegradation and UV light irradiation. Photocatalytic performance of biosynthesized ZnS-NPs was evaluated by the photodegradation of rhodamine

B. In this process, ammonium oxalate and tert-butanol were used as the scavengers of holes and hydroxyl radicals, respectively. ZnS showed high photocatalytic efficiency for RhB degradation, and it was found that the photogenerated holes rather than hydroxyl radicals played the crucial role in the photocatalytic decolorization process. Se nanospheres and nanorods (NRs) reduced by *Lysinibacillus* sp. ZYM-1 were described by Che et al. In this study, photocatalytic performance of Se-NPs was investigated. It is interesting that Se materials showed no significant catalytic effect toward RhB, but the Se nanospheres–H₂O₂ system had higher visible light-driven photocatalytic activity for RhB degradation than Se-NRs. The authors believed that the N-deethylation pathway and chromophore cleavage coexisted. Liquid chromatography high-resolution mass spectrometry results showed that phthalic acid and three N-deethylation intermediates were the products of RhB degradation [90].

3.2. Catalytic Dehalogenation

Chlorinated aromatic compounds are widely used in many industrial applications because of their resistance to oxidation, low water solubility and flame resistance. Overuse of chlorinated aromatic compounds has resulted in the pollution of water, soil, air and sediments. These compounds are persistent and stubborn, making their complete removal quite difficult. While various reductive and oxidative methods have been used for the degradation of chlorinated aromatic compounds, a mild and simple treatment of these stubborn xenobiotics is necessary. It has been proved that biosynthesized Pd-based NPs have excellent performance in the dehalogenation of aromatic compounds. The surfaces of the cells of *Desulfovibrio desulfuricans*, *Desulfovibrio vulgaris* and *Desulfovibrio* sp. 'Oz-7' were used to synthesize Pd-NPs and hydrogen was used as the electron donor. It was proved that the bacteria species affect both the bioreductive efficiency of Pd²⁺ and the dehalogenation performance of Pd-NPs. The highest specific dechlorination rate of bio-Pd-NPs was approximately 30 times greater than that of chemical-Pd-NPs. This difference in catalytic activity was attributed to the favorable effects of the 3-D array, chemical composition and architecture of the functional groups of the Pd-NPs [91].

Another group also biosynthesized Pd-NPs by using *Desulfovibrio desulfuricans* with the same electron donor. The release of chloride was used as the indicator of dehalogenation, and the dehalogenation effect was estimated based on the degradation of polychlorinated biphenyls and 2-chlorophenol biphenyls. For the dehalogenation of 2,3,4,5-tetrachlorobiphenyl, biosynthesized Pd-NPs were used to evaluate the dehalogenation effect in comparison with the chemically reduced control (shown in Figure 6). The chloride release rate of the chemically reduced Pd-NPs was only 5% of that of the biosynthesized Pd-NPs [92]. In another case, Pd-NPs were synthesized both intracellularly and extracellularly by *Shewanella oneidensis* MR-1. In this study, H₂, lactate, pyruvate, ethanol and formate acted as the electron donors. The obtained Pd-NPs exhibited excellent dehalogenation performance towards polychlorinated biphenyl congeners in both liquid and solid conditions. The catalytic performance of 50 mg/L bio-Pd-NPs was comparable to that of 500 mg/L chemical Pd-NP powder [93].

3.3. Degradation of 4-Nitrophenol

4-nitrophenol is a typical nitro-aromatic contaminant from dyes and synthetic pesticides. It can stimulate and inhibit the central nervous system and various nerve endings in humans. The degradation of 4-nitrophenol has been used as a general test for evaluating the catalytic performance of NPs because its degradation can be easily measured by UV-Vis spectroscopy [94,95]. Zhang et al. used the marine bacterium *Bacillus* sp. GP to synthesize Pd/Au-NPs. Subsequently, they evaluated the catalytic activity of the Pd/Au-NPs for the reduction of 4-nitrophenol, but found that it was weaker than that of the chemically synthesized NPs. Therefore, several metal oxides were introduced to improve the catalytic performance, such as Al₂O₃, SiO₂ and Fe₃O₄. The enhancement due to these metal oxides was found to be dose-dependent and can be attributed to the metal ions and formation of an alloy: I. Metal ions of the metal oxides acted as Lewis acids and promoted the reaction.

II. The activity of noble metal sites was perturbed by the possible formation of an alloy [96] (shown in Figure 7). Au-NPs were biosynthesized with *Shewanella oneidensis* MR-1 on rGO under both ambient and culture conditions. Compared with its chemical counterpart, the bio-Au-NPs/rGO showed not only a better promoting effect on the microbial reduction of 4-nitrophenol, but also higher catalytic performance and reusability to the degradation of other contaminants, such as nitrobenzene [97]. The catalytic activity was still maintained at 72% of the initial value after ten reduction cycles. The synergistic effects of rGO and Au-NPs may be responsible for the catalytic activity and reusability of this material as follows: I. rGO provided the template to prevent the Au-NPs from aggregating and increased the concentration of 4-nitrophenol around the Au-NPs on rGO. II. Conductivity of rGO improved the electron transport [98].

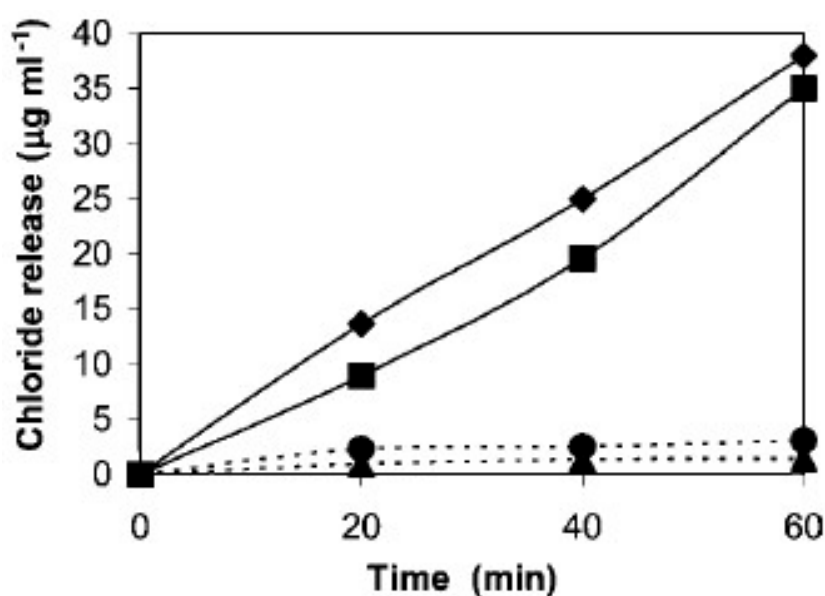


Figure 6. Dehalogenation of 5 mM (aq.) 2-chlorophenol. Solid lines: (♦) Chloride liberation catalyzed by Bio-Pd⁰ and (■) by Chem-Pd⁰. Dashed lines: controls (▲), *Desulfovibrio desulfuricans* cells alone (non-palladized resting cell biomass); (●), finely divided Ref-Pd⁰; data are means from two experiments (reprint from [92] with permission from Springer Nature. Copyright 2004).

3.4. Removal of Heavy Metals Ions

It is well known that the mining industry and the hydrometallurgical industry usually generate a large amount of waste water that contains toxic heavy metal ions [99]. While great efforts have been made to remove these toxicants from polluted water sources that pose a threat to human health, most currently known approaches are costly, and some of these even have side effects on the environment. An increasing number of researchers have been inspired to search for the optimal solution for heavy metal ion removal from the perspective of biology [100,101]. Vanadium (V) and chromium (VI) often coexist in the waste water from vanadium ore smelting. Wang et al. simultaneously reduced the toxic vanadium (V) and chromium (VI) with *Shewanella loihica* PV-4. The enhanced bioreduction of vanadium (V) is always accompanied by decreased Cr (VI) bioreduction. After 27 days of operation, the removal efficiencies of V (V) and Cr (VI) were 71.3% and 91.2%, respectively [102]. Ha et al. used the biosynthesized Pd-NPs to remove Cr⁶⁺ from wastewater. In general, compared with chemically reduced Pd-NPs, biosynthesized nanoscale Pd-NPs have smaller sizes and higher surface-to-volume ratios, so they are expected to have better catalytic performance. However, the catalytic efficiency of bio-Pd-NPs for Cr⁶⁺ reduction without ultrasonic treatment was lower than that of chemically synthesized counterparts. Many studies have elucidated the reductive process of Cr⁶⁺ with bacterially recovered Pd-NPs, and it appears that this approach cannot achieve a high catalytic efficiency and mild extract conditions at the same time (shown in Figure 8).

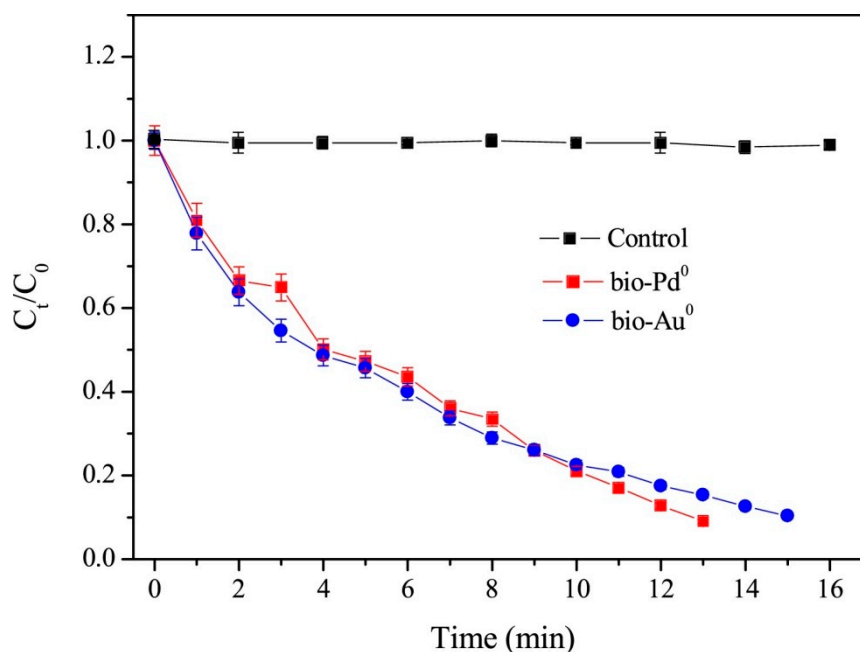


Figure 7. The catalytic performance of bio-Pd-NPs and bio-Au-NPs on 4-NP reduction. (reprint from [96] with permission from Elsevier. Copyright 2018).

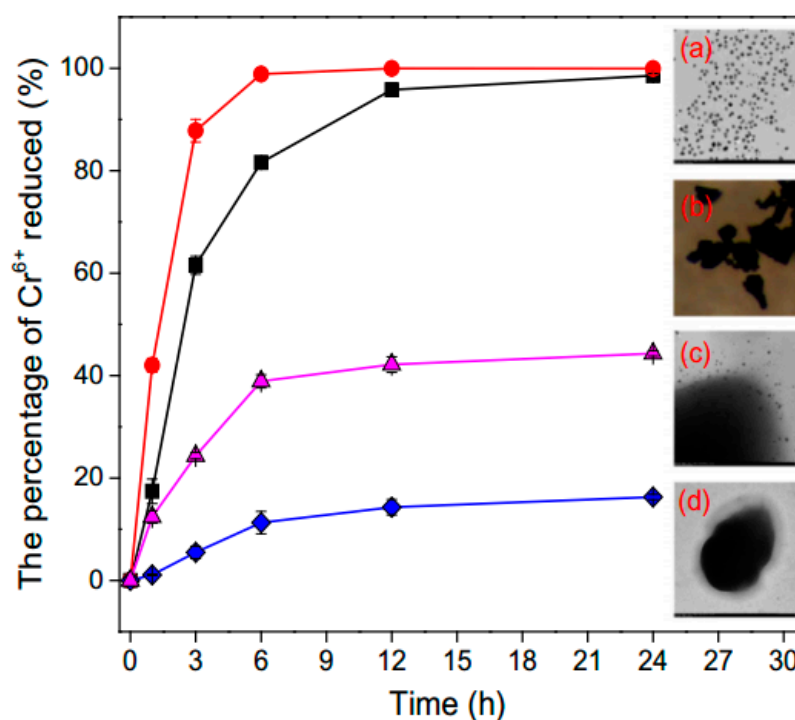


Figure 8. Reduction of 0.5 mM Cr⁶⁺ by ●, sonicated bio-Pd⁰-NPs (a); ■, chem-Pd⁰ (b); ▲, bio-Pd⁰-NPs (c); and ♦, *E. faecalis* cells (d) (reprint from [50] with permission from Elsevier. Copyright 2016).

3.5. Other Catalytic Performance

In addition to the catalytic properties described above, there have been some reports related to other catalytic applications. For example, biosynthesized Pd-NPs were used as catalyst to generate hydrogen from hypophosphite. The catalytic effect was evaluated based on the amount of hydrogen released in this process. In this work, Pd-NPs were obtained by bacteria biomass and cell-free methods.

A high initial release rate of hydrogen was measured just after the addition of hypophosphite to bio-Pd-NPs, and the rate leveled off after approximately 10 minutes. Compared with bacteria biomass control, the cell-free Pd-NPs showed a much higher hydrogen release rate [103]. This difference in the activity was tentatively attributed to the inaccessibility of bio-Pd-NPs fraction embedded in the cell envelope.

In addition, Rostami et al. extensively proved that the electrocatalytic oxidation of hydrazine was significantly promoted by biosynthesized Ag-NPs. Ag-NPs were obtained by reducing the AgNO_3 precursor in the presence of *lead-resistant* MKH1 bacteria. In experiments on the electrochemical oxidation of hydrazine, the authors revealed the relationship between the Ag catalyst content and the current density peak at the forward scan. The results showed that when the Ag-NP content exceeded the threshold value, the current density did not increase because of the aggregation of the Ag-NPs. Chronoamperometry tests and impedance results indicated the excellent catalytic performance and stability of Ag-NPs, indicating that the potential of biosynthesized Ag-NPs in hydrazine fuel cells [104] (shown in Figure 9).

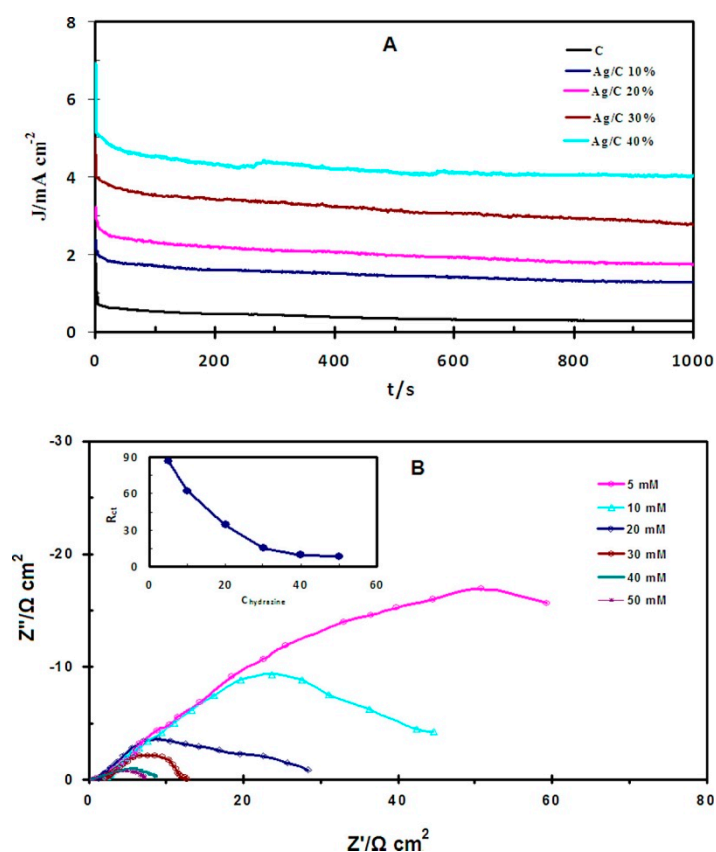


Figure 9. (A) Chronoamperometry curves of Ag/C catalysts with different Ag content in 0.1 M K_2SO_4 + 10 mM N_2H_4 solution at 0.2 V. (B) Nyquist plots recorded at 0.2 V for the Ag/C 40Wt% catalyst in 0.1 M K_2SO_4 containing various hydrazine concentrations. Inset of (B): Plot of the charge transfer resistance (R_{ct}) versus hydrazine concentrations (CN_2H_4). (reprint from [104] with permission from Elsevier. Copyright 2018).

Kimber et al. biosynthesized Cu-NPs intracellularly with *Shewanella oneidensis* MR-1. Many triazole derivatives were synthesized by the Cu^+ catalyzed cycloaddition of benzyl azide to evaluate the catalytic azide-alkyne cycloadditions activity of the Cu-NPs. The authors proposed that Cu_2O shells were formed when Cu-NPs were exposed to air and that the Cu^+ surface layer may be the origin for the excellent catalytic performance. They also proposed that inorganic substances or stabilizing compounds were involved in maintaining superior catalytic activity [105].

4. Conclusion and Outlook

In the past few decades, some special bacteria have been proven to be capable of transforming toxic metal and metalloid ions into functional NPs, becoming known as efficient and eco-friendly nanofactories. This review highlights the NPs synthesized by these specific bacteria and their catalytic applications. Although some mechanisms for bioreduction are still unknown, reasonable hypotheses based on the experimental phenomena have been proposed to provide insight into the fabrication process of the biosynthesized NPs by the bacteria. The biosynthesized NPs were obtained without high-temperature treatments or additional chemicals, and have shown many unique properties, such as catalytic applications, optical applications, aerospace applications, biosensors and gas sensors. More importantly, the conditions for catalysis are usually facile, because bioreduced NPs can catalyze reactions in aqueous media at standard temperature and normal pressure. Due to their biocompatibility and stability, it was also proven that biosynthesized NPs are a feasible alternative to the physical and chemical methods traditionally used in catalysis, particularly in the removal of organic compounds. However, limitations in biosynthesis of NPs still exist: low production, poor control of product quality, contamination from biological cells and difficult separation of NPs from the biological materials.

Further research should focus on the following points: Firstly, a better understanding of the mechanisms involved in the NPs formation is necessary for reproducing biomaterials and controlling the morphology, size and dispersity. Secondly, current studies mainly concentrate on the biosynthesis of Ag, Au, Cu, Pd, Se and Te NPs, while knowledge about other NPs, which have been synthesized by plant, virus or yeast is lacking. Thirdly, exploring the microbial diversity to search for novel and sustainable microorganisms to biosynthesize NPs [106,107]. Finally, in the regard of catalytic applications, effective technologies are needed to separate NPs from medium after catalytic reaction. To explore more characteristics of biosynthesized NPs, novel catalytic applications beyond water treatment and environmental sensors are anticipated.

Author Contributions: This work was initiated by M.D. and Z.J.; under the guidance of Z.W.; X.F. wrote and edited the draft and Y.W. checked the language of manuscript. X.F. and Y.W. contributed equally to this work.

Funding: This research was supported by grants from the Danish National Research Foundation, the AUFF-NOVA project from Aarhus Universitets Forskningsfond and the EU H2020RISE 2016-MNR4S Cell project. Zaixing acknowledges the financial support from National Program for Support of Top-notch Young Professionals, National Natural Science Foundation of China (No. 51773049), China Aerospace Science and Technology Corporation-Harbin Institute of Technology Joint Center for Technology Innovation Fund (HIT15-1A01), Harbin city science and technology projects (2013DB4BP031 and RC2014QN017035), China Postdoctoral Science Special Foundation (No. 201003420, No.20090460067), HIT Research Institute (Zhao Yuan) of New Materials and Intelligent Equipment Technology Co., Ltd. Scientific and Technological Cooperation and Development Fund (No. 2017KJHZ002). Zegao Wang thanks the supporting by the Fundamental Research Funds for the Central Universities, China (YJ201893).

Acknowledgments: X.F. acknowledges the help of Xiaochen Chen in drawing figures.

Conflicts of Interest: The authors declare no conflict of interest.

References

1. Salunke, B.K.; Sawant, S.S.; Lee, S.I.; Kim, B.S. Microorganisms as efficient biosystem for the synthesis of metal nanoparticles: Current scenario and future possibilities. *World J. Microbiol. Biotechnol.* **2016**, *32*, 1–16. [[CrossRef](#)] [[PubMed](#)]
2. Bansal, V.; Rautaray, D.; Bharde, A.; Ahire, K.; Sanyal, A.; Ahmad, A.; Sastry, M. Fungus-mediated biosynthesis of silica and titania particles. *J. Mater. Chem.* **2005**, *15*, 2583–2589. [[CrossRef](#)]
3. Bhushan, M.; Kumar, Y.; Periyasamy, L.; Viswanath, A.K. Facile synthesis of Fe/Zn oxide nanocomposites and study of their structural, magnetic, thermal, antibacterial and cytotoxic properties. *Mater. Chem. Phys.* **2018**, *209*, 233–248. [[CrossRef](#)]
4. Labulo, A.H.; Adesuji, E.T.; Dedeke, O.A.; Bodede, O.S.; Oseghale, C.O.; Moodley, R.; Nyamori, V.O.; Dare, E.O.; Adegoke, O.A. A dual-purpose silver nanoparticles biosynthesized using aqueous leaf extract of *Detarium microcarpum*: An under-utilized species. *Talanta* **2016**, *160*, 735–744. [[CrossRef](#)] [[PubMed](#)]

5. Wang, Z.; Li, Q.; Besenbacher, F.; Dong, M. Facile synthesis of single crystal PtSe₂ nanosheets for nanoscale electronics. *Adv. Mater.* **2016**, *28*, 10224–10229. [[CrossRef](#)] [[PubMed](#)]
6. Wang, Z.; Li, Q.; Xu, H.; Dahl-Petersen, C.; Yang, Q.; Cheng, D.; Cao, D.; Besenbacher, F.; Lauritsen, J.V.; Helveg, S.; et al. Controllable etching of MoS₂ basal planes for enhanced hydrogen evolution through the formation of active edge sites. *Nano Energy* **2018**, *49*, 634–643. [[CrossRef](#)]
7. Ma, L.; Su, W.; Liu, J.X.; Zeng, X.X.; Huang, Z.; Li, W.; Liu, Z.C.; Tang, J.X. Optimization for extracellular biosynthesis of silver nanoparticles by *Penicillium aculeatum* Su1 and their antimicrobial activity and cytotoxic effect compared with silver ions. *Mater. Sci. Eng. C* **2017**, *77*, 963–971. [[CrossRef](#)]
8. Ovais, M.; Ahmad, I.; Khalil, A.T.; Mukherjee, S.; Javed, R.; Ayaz, M.; Raza, A.; Shinwari, Z.K. Wound healing applications of biogenic colloidal silver and gold nanoparticles: Recent trends and future prospects. *Appl. Microbiol. Biotechnol.* **2018**, *102*, 4305–4318. [[CrossRef](#)]
9. Karunakaran, G.; Jagathambal, M.; Gusev, A.; Torres, J.A.L.; Kolesnikov, E.; Kuznetsov, D. Rapid Biosynthesis of AgNPs Using Soil Bacterium *Azotobacter vinelandii* With Promising Antioxidant and Antibacterial Activities for Biomedical Applications. *JOM* **2017**, *69*, 1206–1212. [[CrossRef](#)]
10. Reverberi, A.P.; Kuznetsov, N.T.; Meshalkin, V.P.; Salerno, M.; Fabiano, B. Systematical analysis of chemical methods in metal nanoparticles synthesis. *Theor. Found. Chem. Eng.* **2016**, *50*, 59–66. [[CrossRef](#)]
11. Gopinath, V.; Priyadarshini, S.; Loke, M.F.; Arunkumar, J.; Marsili, E.; MubarakAli, D.; Velusamy, P.; Vadivelu, J. Biogenic synthesis, characterization of antibacterial silver nanoparticles and its cell cytotoxicity. *Arab. J. Chem.* **2017**, *10*, 1107–1117. [[CrossRef](#)]
12. Zhang, P.; Wang, Z.; Liu, L.; Klausen, L.H.; Wang, Y.; Mi, J.L.; Dong, M. Modulation the electronic property of 2D monolayer MoS₂ by amino acid. *Appl. Mater. Today* **2019**, *14*, 151–158. [[CrossRef](#)]
13. Wang, Z.; Li, Q.; Chen, Y.; Cui, B.; Li, Y.; Besenbacher, F.; Dong, M. The ambipolar transport behavior of WSe₂ transistors and its analogue circuits. *NPG Asia Mater.* **2018**, *10*, 703–712. [[CrossRef](#)]
14. Geng, J.; Jefferson, D.A.; Johnson, B.F.G. Exploring the structural complexities of metal-metalloid nanoparticles: The case of Ni-B as catalyst. *Chemistry* **2009**, *15*, 1134–1143. [[CrossRef](#)] [[PubMed](#)]
15. Wang, Z.; Wu, H.H.; Li, Q.; Besenbacher, F.; Zeng, X.C.; Dong, M. Self-scrolling MoS₂ metallic wires. *Nanoscale* **2018**, *10*, 18178–18185. [[CrossRef](#)] [[PubMed](#)]
16. Ulug, B.; Haluk Turkdemir, M.; Cicek, A.; Mete, A. Role of irradiation in the green synthesis of silver nanoparticles mediated by fig (*Ficus carica*) leaf extract. *Spectrochim. Acta Part A Mol. Biomol. Spectrosc.* **2015**, *135*, 153–161. [[CrossRef](#)]
17. Garole, D.J.; Choudhary, B.C.; Paul, D.; Borse, A.U. Sorption and recovery of platinum from simulated spent catalyst solution and refinery wastewater using chemically modified biomass as a novel sorbent. *Environ. Sci. Pollut. Res.* **2018**, *25*, 10911–10925. [[CrossRef](#)] [[PubMed](#)]
18. Nazari, P.; Faramarzi, M.A.; Sepehrizadeh, Z.; Mofid, M.R.; Bazaz, R.D.; Shahverdi, A.R. Biosynthesis of bismuth nanoparticles using *Serratia marcescens* isolated from the Caspian Sea and their characterisation. *IET Nanobiotechnol.* **2012**, *6*, 58. [[CrossRef](#)]
19. Reverberi, A.P.; Vocciante, M.; Lunghi, E.; Pietrelli, L.; Fabiano, B. New trends in the synthesis of nanoparticles by green methods. *Chem. Eng. Trans.* **2017**, *61*, 667–672. [[CrossRef](#)]
20. Shukla, A.K.; Iravani, S. Metallic nanoparticles: Green synthesis and spectroscopic characterization. *Environ. Chem. Lett.* **2017**, *15*, 223–231. [[CrossRef](#)]
21. Wen, X.; Du, C.; Zeng, G.; Huang, D.; Zhang, J.; Yin, L.; Tan, S.; Huang, L.; Chen, H.; Yu, G.; et al. A novel biosorbent prepared by immobilized *Bacillus licheniformis* for lead removal from wastewater. *Chemosphere* **2018**, *200*, 173–179. [[CrossRef](#)] [[PubMed](#)]
22. Won, S.W.; Mao, J.; Kwak, I.S.; Sathishkumar, M.; Yun, Y.S. Platinum recovery from ICP wastewater by a combined method of biosorption and incineration. *Bioresour. Technol.* **2010**, *101*, 1135–1140. [[CrossRef](#)] [[PubMed](#)]
23. Xiang, L.; Wei, J.; Jianbo, S.; Guili, W.; Feng, G.; Ying, L. Purified and sterilized magnetosomes from *Magnetospirillum gryphiswaldense* MSR-1 were not toxic to mouse fibroblasts in vitro. *Lett. Appl. Microbiol.* **2007**, *45*, 75–81. [[CrossRef](#)] [[PubMed](#)]
24. Saravana Kumar, P.; Balachandran, C.; Duraipandiyar, V.; Ramasamy, D.; Ignacimuthu, S.; Al-Dhabi, N.A. Extracellular biosynthesis of silver nanoparticle using *Streptomyces* sp. 09 PBT 005 and its antibacterial and cytotoxic properties. *Appl. Nanosci.* **2015**, *5*, 169–180. [[CrossRef](#)]

25. Verma, S.K.; Jha, E.; Panda, P.K.; Mishra, A.; Thirumurugan, A.; Das, B.; Parashar, S.K.S.; Suar, M. Rapid novel facile biosynthesized silver nanoparticles from bacterial release induce biogenicity and concentration dependent in vivo cytotoxicity with embryonic Zebrafish-A mechanistic insight. *Toxicol. Sci.* **2018**, *161*, 125–138. [[CrossRef](#)] [[PubMed](#)]
26. Tamboli, D.P.; Lee, D.S. Mechanistic antimicrobial approach of extracellularly synthesized silver nanoparticles against gram positive and gram negative bacteria. *J. Hazard. Mater.* **2013**, *260*, 878–884. [[CrossRef](#)] [[PubMed](#)]
27. Ma, B.; Kong, C.; Hu, X.; Liu, K.; Huang, Q.; Lv, J.; Lu, W.; Zhang, X.; Yang, Z.; Yang, S. A sensitive electrochemical nonenzymatic biosensor for the detection of H₂O₂ released from living cells based on ultrathin concave Ag nanosheets. *Biosens. Bioelectron.* **2018**, *106*, 29–36. [[CrossRef](#)]
28. Naim, M.M.; El-Shafei, A.A.; Elewa, M.M.; Moneer, A.A. Application of silver-, iron-, and chitosan-nanoparticles in wastewater treatment. *Int. Conf. Eur. Desalin. Soc. Desalin. Environ. Clean Water Energy* **2016**, *73*, 268–280. [[CrossRef](#)]
29. Liu, W.; Tian, S.; Zhao, X.; Xie, W.; Gong, Y.; Zhao, D. Application of Stabilized Nanoparticles for In Situ Remediation of Metal-Contaminated Soil and Groundwater: A Critical Review. *Curr. Pollut. Rep.* **2015**, *1*, 280–291. [[CrossRef](#)]
30. Vanalakar, S.A.; Patil, P.S.; Kim, J.H. Recent advances in synthesis of Cu₂FeSn₄ materials for solar cell applications: A review. *Sol. Energy Mater. Sol. Cells* **2018**, *182*, 204–219. [[CrossRef](#)]
31. Pantidos, N. Biological Synthesis of Metallic Nanoparticles by Bacteria, Fungi and Plants. *J. Nanomed. Nanotechnol.* **2014**, *5*, 233. [[CrossRef](#)]
32. Ahmed, S.; Annu, Ikram, S.; Yudha, S. Biosynthesis of gold nanoparticles: A green approach. *J. Photochem. Photobiol. B Biol.* **2016**, *161*, 141–153. [[CrossRef](#)] [[PubMed](#)]
33. Timoszyk, A.; Niedbach, J.; Śliżewska, P.; Mirończyk, A.; Kozioł, J.J. Eco-Friendly and Temperature Dependent Biosynthesis of Gold Nanoparticles Using the Bacterium *Pseudomonas aeruginosa*: Characterization and Antibacterial Activity. *J. Nano Res.* **2017**, *48*, 114–124. [[CrossRef](#)]
34. Mekkawy, A.I.; El-Mokhtar, M.A.; Nafady, N.A.; Yousef, N.; Hamad, M.; El-Shanawany, S.M.; Ibrahim, E.H.; Elsabahy, M. In vitro and in vivo evaluation of biologically synthesized silver nanoparticles for topical applications: Effect of surface coating and loading into hydrogels. *Int. J. Nanomed.* **2017**, *12*, 759–777. [[CrossRef](#)] [[PubMed](#)]
35. Siddiqi, K.S.; Husen, A.; Rao, R.A.K. A review on biosynthesis of silver nanoparticles and their biocidal properties. *J. Nanobiotechnol.* **2018**, *16*. [[CrossRef](#)] [[PubMed](#)]
36. Klaus, T.; Joerger, R.; Olsson, E.; Granqvist, C.-G. Silver-based crystalline nanoparticles, microbially fabricated. *Proc. Natl. Acad. Sci. USA* **1999**, *96*, 13611–13614. [[CrossRef](#)] [[PubMed](#)]
37. Pereira, L.; Mehboob, F.; Stams, A.J.M.; Mota, M.M.; Rijnaarts, H.H.M.; Alves, M.M. Metallic nanoparticles: Microbial synthesis and unique properties for biotechnological applications, bioavailability and biotransformation. *Crit. Rev. Biotechnol.* **2015**, *35*, 114–128. [[CrossRef](#)]
38. Ghiuță, I.; Cristea, D.; Croitoru, C.; Kost, J.; Wenkert, R.; Vyrides, I.; Anayiotos, A.; Munteanu, D. Characterization and antimicrobial activity of silver nanoparticles, biosynthesized using *Bacillus* species. *Appl. Surf. Sci.* **2018**, *438*, 66–73. [[CrossRef](#)]
39. Yurtluk, T.; Akçay, F.A.; Avcı, A. Biosynthesis of silver nanoparticles using novel *Bacillus* sp. SBT8. *Prep. Biochem. Biotechnol.* **2018**, *48*, 151–159. [[CrossRef](#)]
40. Mishra, S.; Singh, B.R.; Naqvi, A.H.; Singh, H.B. Potential of biosynthesized silver nanoparticles using *Stenotrophomonas* sp. BHU-S7 (MTCC 5978) for management of soil-borne and foliar phytopathogens. *Sci. Rep.* **2017**, *7*, 1–15. [[CrossRef](#)]
41. Li, J.; Tian, B.; Li, T.; Dai, S.; Weng, Y.; Lu, J.; Xu, X.; Jin, Y.; Pang, R.; Hua, Y. Biosynthesis of Au, Ag and Au–Ag bimetallic nanoparticles using protein extracts of *Deinococcus radiodurans* and evaluation of their cytotoxicity. *Int. J. Nanomed.* **2018**, *13*, 1411–1424. [[CrossRef](#)] [[PubMed](#)]
42. Wadhvani, S.A.; Shedbalkar, U.U.; Singh, R.; Chopade, B.A. Biosynthesis of gold and selenium nanoparticles by purified protein from *Acinetobacter* sp. SW 30. *Enzyme Microb. Technol.* **2018**, *111*, 81–86. [[CrossRef](#)] [[PubMed](#)]
43. Li, J.; Li, Q.; Ma, X.; Tian, B.; Li, T.; Yu, J.; Dai, S.; Weng, Y.; Hua, Y. Biosynthesis of gold nanoparticles by the extreme bacterium *Deinococcus radiodurans* and an evaluation of their antibacterial properties. *Int. J. Nanomed.* **2016**, *11*, 5931–5944. [[CrossRef](#)] [[PubMed](#)]

44. Nair, B.; Pradeep, T. Coalescence of Nanoclusters and Formation of Submicron Crystallites Assisted by Lactobacillus Strains. *Cryst. Growth Des.* **2002**, *2*, 293–298. [[CrossRef](#)]
45. Suresh, A.K.; Pelletier, D.A.; Wang, W.; Moon, J.-W.; Gu, B.; Mortensen, N.P.; Allison, D.P.; Joy, D.C.; Phelps, T.J.; Doktycz, M.J. Silver Nanocrystallites: Biofabrication using *Shewanella oneidensis*, and an Evaluation of Their Comparative Toxicity on Gram-negative and Gram-positive Bacteria. *Environ. Sci. Technol.* **2010**, *44*, 5210–5215. [[CrossRef](#)] [[PubMed](#)]
46. Venil, C.K.; Sathishkumar, P.; Malathi, M.; Usha, R.; Jayakumar, R.; Yusoff, A.R.M.; Ahmad, W.A. Synthesis of flexirubin-mediated silver nanoparticles using *Chryseobacterium artocarpi* CECT 8497 and investigation of its anticancer activity. *Mater. Sci. Eng. C* **2016**, *59*, 228–234. [[CrossRef](#)] [[PubMed](#)]
47. Lv, Q.; Zhang, B.; Xing, X.; Zhao, Y.; Cai, R.; Wang, W.; Gu, Q. Biosynthesis of copper nanoparticles using *Shewanella loihica* PV-4 with antibacterial activity: Novel approach and mechanisms investigation. *J. Hazard. Mater.* **2018**, *347*, 141–149. [[CrossRef](#)]
48. Abirami, M.; Kannabiran, K. *Streptomyces ghanaensis* VITHM1 mediated green synthesis of silver nanoparticles: Mechanism and biological applications. *Front. Chem. Sci. Eng.* **2016**, *10*, 542–551. [[CrossRef](#)]
49. Kimber, R.L.; Lewis, E.A.; Parmeggiani, F.; Smith, K.; Bagshaw, H.; Starborg, T.; Joshi, N.; Figueroa, A.I.; van der Laan, G.; Cibir, G.; et al. Biosynthesis and Characterization of Copper Nanoparticles Using *Shewanella oneidensis*: Application for Click Chemistry. *Small* **2018**, *14*, 1–8. [[CrossRef](#)]
50. Ha, C.; Zhu, N.; Shang, R.; Shi, C.; Cui, J.; Sohoo, I.; Wu, P.; Cao, Y. Biorecovery of palladium as nanoparticles by *Enterococcus faecalis* and its catalysis for chromate reduction. *Chem. Eng. J.* **2016**, *288*, 246–254. [[CrossRef](#)]
51. Dong, Z.Y.; Rao, M.P.N.; Xiao, M.; Wang, H.F.; Hozzein, W.N.; Chen, W.; Li, W.J. Antibacterial activity of silver nanoparticles against *Staphylococcus warneri* synthesized using endophytic bacteria by photo-irradiation. *Front. Microbiol.* **2017**, *8*, 1–8. [[CrossRef](#)] [[PubMed](#)]
52. Tian, L.-J.; Li, W.-W.; Zhu, T.-T.; Chen, J.-J.; Wang, W.-K.; An, P.-F.; Zhang, L.; Dong, J.-C.; Guan, Y.; Liu, D.-F.; et al. Directed Biofabrication of Nanoparticles through Regulating Extracellular Electron Transfer. *J. Am. Chem. Soc.* **2017**, *139*, 12149–12152. [[CrossRef](#)] [[PubMed](#)]
53. Forootanfar, H.; Amirpour-Rostami, S.; Jafari, M.; Forootanfar, A.; Yousefizadeh, Z.; Shakibaie, M. Microbial-assisted synthesis and evaluation the cytotoxic effect of tellurium nanorods. *Mater. Sci. Eng. C* **2015**, *49*, 183–189. [[CrossRef](#)] [[PubMed](#)]
54. Cheng, Y.; Xiao, X.; Li, X.; Song, D.; Lu, Z.; Wang, F.; Wang, Y. Characterization, antioxidant property and cytoprotection of exopolysaccharide-capped elemental selenium particles synthesized by *Bacillus paralicheniformis* SR14. *Carbohydr. Polym.* **2017**, *178*, 18–26. [[CrossRef](#)] [[PubMed](#)]
55. Shoeibi, S.; Mozdziak, P.; Golkar-Narenji, A. Biogenesis of Selenium Nanoparticles Using Green Chemistry. *Top. Curr. Chem.* **2017**, *375*, 1–21. [[CrossRef](#)]
56. Dias, D.A.; Kouremenos, K.A.; Beale, D.J.; Callahan, D.L.; Jones, O.A.H. Metal and metalloid containing natural products and a brief overview of their applications in biology, biotechnology and biomedicine. *BioMetals* **2016**, *29*, 1–13. [[CrossRef](#)]
57. Presentato, A.; Piacenza, E.; Anikovskiy, M.; Cappelletti, M.; Zannoni, D.; Turner, R.J. Biosynthesis of selenium-nanoparticles and -nanorods as a product of selenite bioconversion by the aerobic bacterium *Rhodococcus aetherivorans* BCP1. *New Biotechnol.* **2018**, *41*, 1–8. [[CrossRef](#)]
58. Song, D.; Li, X.; Cheng, Y.; Xiao, X.; Lu, Z.; Wang, Y.; Wang, F. Aerobic biogenesis of selenium nanoparticles by *Enterobacter cloacae* Z0206 as a consequence of fumarate reductase mediated selenite reduction. *Sci. Rep.* **2017**, *7*, 19–21. [[CrossRef](#)]
59. Xu, C.; Qiao, L.; Guo, Y.; Ma, L.; Cheng, Y. Preparation, characteristics and antioxidant activity of polysaccharides and proteins-capped selenium nanoparticles synthesized by *Lactobacillus casei* ATCC 393. *Carbohydr. Polym.* **2018**, *195*, 576–585. [[CrossRef](#)]
60. Wang, X.; Zhang, D.; Pan, X.; Lee, D.J.; Al-Misned, F.A.; Mortuza, M.G.; Gadd, G.M. Aerobic and anaerobic biosynthesis of nano-selenium for remediation of mercury contaminated soil. *Chemosphere* **2017**, *170*, 266–273. [[CrossRef](#)]
61. Avendaño, R.; Chaves, N.; Fuentes, P.; Sánchez, E.; Jiménez, J.I.; Chavarría, M. Production of selenium nanoparticles in *Pseudomonas putida* KT2440. *Sci. Rep.* **2016**, *6*, 1–9. [[CrossRef](#)] [[PubMed](#)]
62. Zonaro, E.; Lampis, S.; Turner, R.J.; Junaid, S.; Vallini, G. Biogenic selenium and tellurium nanoparticles synthesized by environmental microbial isolates efficaciously inhibit bacterial planktonic cultures and biofilms. *Front. Microbiol.* **2015**, *6*, 1–11. [[CrossRef](#)] [[PubMed](#)]

63. Srivastava, P.; Nikhil, E.V.R.; Bragança, J.M.; Kowshik, M. Anti-bacterial TeNPs biosynthesized by haloarchaeon *Halococcus salifodinae* BK3. *Extremophiles* **2015**, *19*, 875–884. [[CrossRef](#)] [[PubMed](#)]
64. Presentato, A.; Piacenza, E.; Anikovskiy, M.; Cappelletti, M.; Zannoni, D.; Turner, R.J. *Rhodococcus aetherivorans* BCP1 as cell factory for the production of intracellular tellurium nanorods under aerobic conditions. *Microb. Cell Fact.* **2016**, *15*, 1–14. [[CrossRef](#)] [[PubMed](#)]
65. Jeevanandam, J.; Barhoum, A.; Chan, Y.S.; Dufresne, A.; Danquah, M.K. Review on nanoparticles and nanostructured materials: History, sources, toxicity and regulations. *Beilstein J. Nanotechnol.* **2018**, *9*, 1050–1074. [[CrossRef](#)] [[PubMed](#)]
66. Fabricius, A.L.; Duester, L.; Ecker, D.; Ternes, T.A. Metal and metalloid size-fractionation strategies in spatial high-resolution sediment pore water profiles. *Environ. Sci. Technol.* **2016**, *50*, 9506–9514. [[CrossRef](#)]
67. Obayemi, J.D.; Dozie-Nwachukwu, S.; Danyuo, Y.; Odusanya, O.S.; Anuku, N.; Malatesta, K.; Soboyejo, W.O. Biosynthesis and the conjugation of magnetite nanoparticles with luteinizing hormone releasing hormone (LHRH). *Mater. Sci. Eng. C* **2015**, *46*, 482–496. [[CrossRef](#)]
68. Rajendran, K.; Karunakaran, V.; Mahanty, B.; Sen, S. Biosynthesis of hematite nanoparticles and its cytotoxic effect on HepG2 cancer cells. *Int. J. Biol. Macromol.* **2015**, *74*, 376–381. [[CrossRef](#)]
69. Saif, S.; Tahir, A.; Chen, Y. Green Synthesis of Iron Nanoparticles and Their Environmental Applications and Implications. *Nanomaterials* **2016**, *6*, 209. [[CrossRef](#)]
70. Srivastava, N.; Mukhopadhyay, M. Biosynthesis of SnO₂ Nanoparticles Using Bacterium *Erwinia herbicola* and Their Photocatalytic Activity for Degradation of Dyes. *Ind. Eng. Chem. Res.* **2014**, *53*, 13971–13979. [[CrossRef](#)]
71. Ghasemi, N.; Jamali-Sheini, F.; Zekavati, R. CuO and Ag/CuO nanoparticles: Biosynthesis and antibacterial properties. *Mater. Lett.* **2017**, *196*, 78–82. [[CrossRef](#)]
72. Bakhshi, M.; Hosseini, M.R. Synthesis of CdS nanoparticles from cadmium sulfate solutions using the extracellular polymeric substances of *B. licheniformis* as stabilizing agent. *Enzyme Microb. Technol.* **2016**, *95*, 209–216. [[CrossRef](#)] [[PubMed](#)]
73. Yan, Z.Y.; Du, Q.Q.; Qian, J.; Wan, D.Y.; Wu, S.M. Eco-friendly intracellular biosynthesis of CdS quantum dots without changing *Escherichia coli*'s antibiotic resistance. *Enzyme Microb. Technol.* **2017**, *96*, 96–102. [[CrossRef](#)]
74. Sakimoto, K.K.; Wong, A.B.; Yang, P. Self-photosensitization of nonphotosynthetic bacteria for solar-to-chemical production. *Science* **2016**, *351*, 74–77. [[CrossRef](#)] [[PubMed](#)]
75. Qi, P.; Zhang, D.; Zeng, Y.; Wan, Y. Biosynthesis of CdS nanoparticles: A fluorescent sensor for sulfate-reducing bacteria detection. *Talanta* **2016**, *147*, 142–146. [[CrossRef](#)] [[PubMed](#)]
76. Kominkova, M.; Milosavljevic, V.; Vitek, P.; Polanska, H.; Cihalova, K.; Dostalova, S.; Hynstova, V.; Guran, R.; Kopel, P.; Richtera, L.; et al. Comparative study on toxicity of extracellularly biosynthesized and laboratory synthesized CdTe quantum dots. *J. Biotechnol.* **2017**, *241*, 193–200. [[CrossRef](#)] [[PubMed](#)]
77. Yue, L.; Wang, J.; Zhang, Y.; Qi, S.; Xin, B. Controllable biosynthesis of high-purity lead-sulfide (PbS) nanocrystals by regulating the concentration of polyethylene glycol in microbial system. *Bioprocess Biosyst. Eng.* **2016**, *39*, 1839–1846. [[CrossRef](#)]
78. Srivastava, P.; Kowshik, M. Fluorescent Lead(IV) Sulfide Nanoparticles Synthesized by *Idiomarina* sp. Strain PR58-8 for Bioimaging Applications. *Appl. Environ. Microbiol.* **2017**, *83*, e03091-16. [[CrossRef](#)]
79. Xiao, X.; Liu, Q.-Y.; Lu, X.-R.; Li, T.-T.; Feng, X.-L.; Li, Q.; Liu, Z.-Y.; Feng, Y.-J. Self-assembly of complex hollow CuS nano/micro shell by an electrochemically active bacterium *Shewanella oneidensis* MR-1. *Int. Biodeterior. Biodegrad.* **2017**, *116*, 10–16. [[CrossRef](#)]
80. Zhou, N.Q.; Tian, L.J.; Wang, Y.C.; Li, D.B.; Li, P.P.; Zhang, X.; Yu, H.Q. Extracellular biosynthesis of copper sulfide nanoparticles by *Shewanella oneidensis* MR-1 as a photothermal agent. *Enzym. Microb. Technol.* **2016**, *95*, 230–235. [[CrossRef](#)]
81. Xiao, X.; Ma, X.B.; Yuan, H.; Liu, P.C.; Lei, Y.B.; Xu, H.; Du, D.L.; Sun, J.F.; Feng, Y.J. Photocatalytic properties of zinc sulfide nanocrystals biofabricated by metal-reducing bacterium *Shewanella oneidensis* MR-1. *J. Hazard. Mater.* **2015**, *288*, 134–139. [[CrossRef](#)] [[PubMed](#)]
82. Qi, S.; Zhang, M.; Guo, X.; Yue, L.; Wang, J.; Shao, Z.; Xin, B. Controlled extracellular biosynthesis of ZnS quantum dots by sulphate reduction bacteria in the presence of hydroxypropyl starch as a mediator. *J. Nanopart. Res.* **2017**, *19*. [[CrossRef](#)]

83. Doshi, B.; Sillanpää, M.; Kalliola, S. A review of bio-based materials for oil spill treatment. *Water Res.* **2018**, *135*, 262–277. [[CrossRef](#)] [[PubMed](#)]
84. Hu, X.; Ren, C.; Kang, W.; Mu, L.; Liu, X.; Li, X.; Wang, T.; Zhou, Q. Characterization and toxicity of nanoscale fragments in wastewater treatment plant effluent. *Sci. Total Environ.* **2018**, *626*, 1332–1341. [[CrossRef](#)] [[PubMed](#)]
85. Schröfel, A.; Kratošová, G.; Šafařík, I.; Šafaříková, M.; Raška, I.; Shor, L.M. Applications of biosynthesized metallic nanoparticles—A review. *Acta Biomater.* **2014**, *10*, 4023–4042. [[CrossRef](#)] [[PubMed](#)]
86. Choi, S.; Johnston, M.; Wang, G.S.; Huang, C.P. A seasonal observation on the distribution of engineered nanoparticles in municipal wastewater treatment systems exemplified by TiO₂ and ZnO. *Sci. Total Environ.* **2018**, *625*, 1321–1329. [[CrossRef](#)] [[PubMed](#)]
87. Seifan, M.; Ebrahimezhad, A.; Ghasemi, Y.; Samani, A.K.; Berenjian, A. The role of magnetic iron oxide nanoparticles in the bacterially induced calcium carbonate precipitation. *Appl. Microbiol. Biotechnol.* **2018**, *102*, 3595–3606. [[CrossRef](#)] [[PubMed](#)]
88. Huang, Z.; Zeng, Z.; Chen, A.; Zeng, G.; Xiao, R.; Xu, P.; He, K.; Song, Z.; Hu, L.; Peng, M.; et al. Differential behaviors of silver nanoparticles and silver ions towards cysteine: Bioremediation and toxicity to *Phanerochaete chrysosporium*. *Chemosphere* **2018**, *203*, 199–208. [[CrossRef](#)]
89. Zhang, Y.; Qiang, L.; Yuan, Y.; Wu, W.; Sun, B.; Zhu, L. Impacts of titanium dioxide nanoparticles on transformation of silver nanoparticles in aquatic environments. *Environ. Sci. Nano* **2018**, *5*, 1191–1199. [[CrossRef](#)]
90. Che, L.; Dong, Y.; Wu, M.; Zhao, Y.; Liu, L.; Zhou, H. Characterization of Selenite Reduction by *Lysinibacillus* sp. ZYM-1 and Photocatalytic Performance of Biogenic Selenium Nanospheres. *ACS Sustain. Chem. Eng.* **2017**, *5*, 2535–2543. [[CrossRef](#)]
91. Baxter-Plant, V.S.; Mikheenko, I.P.; Macaskie, L.E. Sulphate-reducing bacteria, palladium and the reductive dehalogenation of chlorinated aromatic compounds. *Biodegradation* **2003**, *14*, 83–90. [[CrossRef](#)] [[PubMed](#)]
92. Baxter-Plant, V.S.; Mikheenko, I.P.; Robson, M.; Harrad, S.J.; Macaskie, L.E. Dehalogenation of chlorinated aromatic compounds using a hybrid bioinorganic catalyst on cells of *Desulfovibrio desulfuricans*. *Biotechnol. Lett.* **2004**, *26*, 1885–1890. [[CrossRef](#)] [[PubMed](#)]
93. De Windt, W.; Aelterman, P.; Verstraete, W. Bioreductive deposition of palladium (0) nanoparticles on *Shewanella oneidensis* with catalytic activity towards reductive dechlorination of polychlorinated biphenyls. *Environ. Microbiol.* **2005**, *7*, 314–325. [[CrossRef](#)] [[PubMed](#)]
94. Hosseinpour, M.; Fatemi, S.; Ahmadi, S.J.; Morimoto, M.; Akizuki, M.; Oshima, Y.; Fumoto, E. The synergistic effect between supercritical water and redox properties of iron oxide nanoparticles for in-situ catalytic upgrading heavy oil with formic acid. Isotopic study. *Appl. Catal. B Environ.* **2018**, *230*, 91–101. [[CrossRef](#)]
95. Zhang, H.; Hu, X. Rapid production of Pd nanoparticle by a marine electrochemically active bacterium: *Shewanella* sp. CNZ-1 and its catalytic performance on 4-nitrophenol reduction. *RSC Adv.* **2017**, *7*, 41182–41189. [[CrossRef](#)]
96. Zhang, H.; Hu, X. Biosynthesis of Pd and Au as nanoparticles by a marine bacterium *Bacillus* sp. GP and their enhanced catalytic performance using metal oxides for 4-nitrophenol reduction. *Enzyme Microb. Technol.* **2018**, *113*, 59–66. [[CrossRef](#)]
97. Cumbal, L.; Greenleaf, J.; Leun, D.; SenGupta, A.K. Polymer supported inorganic nanoparticles: Characterization and environmental applications. *React. Funct. Polym.* **2003**, *54*, 167–180. [[CrossRef](#)]
98. Dong, B.; Liu, G.; Zhou, J.; Wang, A.; Wang, J.; Jin, R.; Lv, H. Biogenic gold nanoparticles-reduced graphene oxide nanohybrid: Synthesis, characterization and application in chemical and biological reduction of nitroaromatics. *RSC Adv.* **2015**, *5*, 97798–97806. [[CrossRef](#)]
99. Rüdél, H.; Díaz Muñoz, C.; Garelick, H.; Kandile, N.G.; Miller, B.W.; Pantoja Muñoz, L.; Peijnenburg, W.J.G.M.; Purchase, D.; Shevah, Y.; van Sprang, P.; et al. Consideration of the bioavailability of metal/metalloid species in freshwaters: Experiences regarding the implementation of biotic ligand model-based approaches in risk assessment frameworks. *Environ. Sci. Pollut. Res.* **2015**, *22*, 7405–7421. [[CrossRef](#)]
100. Vilela, P.; Liu, H.; Lee, S.C.; Hwangbo, S.; Nam, K.J.; Yoo, C.K. A systematic approach of removal mechanisms, control and optimization of silver nanoparticle in wastewater treatment plants. *Sci. Total Environ.* **2018**, *633*, 989–998. [[CrossRef](#)]

101. Vilardi, G.; Mpouras, T.; Dermatas, D.; Verdone, N.; Polydera, A.; Di Palma, L. Nanomaterials application for heavy metals recovery from polluted water: The combination of nano zero-valent iron and carbon nanotubes. Competitive adsorption non-linear modeling. *Chemosphere* **2018**, *201*, 716–729. [[CrossRef](#)] [[PubMed](#)]
102. Wang, G.; Zhang, B.; Li, S.; Yang, M.; Yin, C. Simultaneous microbial reduction of vanadium (V) and chromium (VI) by *Shewanella loihica* PV-4. *Bioresour. Technol.* **2017**, *227*, 353–358. [[CrossRef](#)] [[PubMed](#)]
103. Bunge, M.; Søbberg, L.S.; Rotaru, A.E.; Gauthier, D.; Lindhardt, A.T.; Hause, G.; Finster, K.; Kingshott, P.; Skrydstrup, T.; Meyer, R.L. Formation of palladium(0) nanoparticles at microbial surfaces. *Biotechnol. Bioeng.* **2010**, *107*, 206–215. [[CrossRef](#)] [[PubMed](#)]
104. Rostami, H.; Khosravi, F.; Mohseni, M.; Rostami, A.A. Biosynthesis of Ag nanoparticles using isolated bacteria from contaminated sites and its application as an efficient catalyst for hydrazine electrooxidation. *Int. J. Biol. Macromol.* **2018**, *107*, 343–348. [[CrossRef](#)]
105. Velmurugan, P.; Hong, S.C.; Aravinthan, A.; Jang, S.H.; Yi, P.I.; Song, Y.C.; Jung, E.S.; Park, J.S.; Sivakumar, S. Comparison of the Physical Characteristics of Green-Synthesized and Commercial Silver Nanoparticles: Evaluation of Antimicrobial and Cytotoxic Effects. *Arab. J. Sci. Eng.* **2017**, *42*, 201–208. [[CrossRef](#)]
106. Pfeffer, C.; Larsen, S.; Song, J.; Dong, M.; Besenbacher, F.; Meyer, R.L.; Kjeldsen, K.U.; Schreiber, L.; Gorby, Y.A.; El-Naggar, M.Y.; et al. Filamentous bacteria transport electrons over centimetre distances. *Nature* **2012**, *491*, 218–221. [[CrossRef](#)]
107. Jiang, Z.; Zhang, S.; Klausen, L.H.; Song, J.; Li, Q.; Wang, Z.; Stokke, B.T.; Huang, Y.; Besenbacher, F.; Nielsen, L.P.; et al. In vitro single-cell dissection revealing the interior structure of cable bacteria. *Proc. Natl. Acad. Sci. USA* **2018**, *115*, 8515–8522. [[CrossRef](#)]



© 2019 by the authors. Licensee MDPI, Basel, Switzerland. This article is an open access article distributed under the terms and conditions of the Creative Commons Attribution (CC BY) license (<http://creativecommons.org/licenses/by/4.0/>).